Manganese is a Deinococcus radiodurans growth limiting factor in rich culture medium

Manganese is a *Deinococcus radiodurans* growth limiting factor in rich culture medium

Francesca Borsetti°, Fabrizio Dal Piaz$, Federico D'Alessio•, Alessandra Stefan•^, Renato Brandimarti•, Anindita Sarkar£, Ankona Datta£, Alejandro Montón Silva§, Tanneke den Blaauwen§, Mucchi Alberto*, Enzo Spisni°, Alejandro Hochkoeppler•^#

° Department of Biology, Geology and Environmental Sciences, Via Selmi 3, 40125 Bologna (Italy)

• Department of Pharmacy and Biotechnology, Viale Risorgimento 4, 40136 Bologna (Italy)

$ Department of Medicine, University of Salerno, Via Giovanni Paolo II 132, 84084 Fisciano SA (Italy)

£ Department of Chemical Sciences, Tata Institute of Fundamental Research, Mumbai 400005 (India)

§ Bacterial Cell Biology & Physiology, Swammerdam Institute for Life Sciences, University of Amsterdam, Science Park 904, 1098 XH Amsterdam (The Netherlands)

*Department of Industrial Chemistry "Toson Montanari", University of Bologna, Viale Risorgimento 4, 40136 Bologna (Italy)

^ CSGI, University of Firenze, Via della Lastruccia 3, 50019 Sesto Fiorentino FI (Italy),

#To whom correspondence should be addressed:

Prof. Alejandro Hochkoeppler
Department of Pharmacy and Biotechnology
University of Bologna
Viale Risorgimento 4
40136 Bologna
Italy
Tel.: ++ 39 051 2093671
Fax: ++ 39 051 2093673
e-mail: a.hochkoeppler@unibo.it

Subject category: physiology and metabolism.

Key words: *Deinococcus radiodurans*; manganese; growth; proteome.

Word count: Abstract: 241; Text: 5006; Total: 5247.

Abbreviations: TGY: tryptone, glucose, yeast extract; BODIPY: boron dipyrromethene; TBS: Tris-Buffered-Saline; PBS: Phosphate-Buffered-Saline; EMCDD: electron multiplying charge-coupled-camera; CHAPS: 3-[(3-cholamidopropyl)dimethylammonio]-1-propanesulfonate; EDTA: ethylenediaminetetraacetic acid; IPG: immobilized pH gradient; DTT: 1,4-dithiothreitol; MS: mass spectrometry; LC-MS: liquid chromatography – mass spectrometry.

ABSTRACT

To understand the effects triggered by Mn^{2+} on *Deinococcus radiodurans*, the proteome patterns associated to different growth phases were investigated. In particular, we tested under physiological conditions the growth rate and the biomass yield of *D. radiodurans* cultured in rich medium supplemented or not with $MnCl_2$. The addition to the medium of 2.5-5.0 μM $MnCl_2$ did neither alter the growth rate nor the lag phase, but significantly increased biomass yield. When higher $MnCl_2$ concentrations were used (10-250 μM), biomass was again found to be positively affected, although we did observe a concentration-dependent increase of the lag phase. The *in vivo* concentration of Mn^{2+} was determined in cells grown in rich medium supplemented or not with 5 μM $MnCl_2$. By atomic absorption spectroscopy we estimated 0.2 and 0.75 mM Mn^{2+} concentration in cells grown in control and enriched medium, respectively. We qualitatively confirmed this observation using a fluorescent turn-on sensor designed to selectively detect Mn^{2+} *in vivo*. Finally, we investigated the proteome composition of cells grown for 15 or 19 h in medium to which 5 μM $MnCl_2$ was added, and we compared these proteomes with those of cells grown in control medium. The presence of 5 μM $MnCl_2$ in the culture medium was found to alter the pI of some proteins, suggesting that manganese affects post-translational modifications. Further, we observed that Mn^{2+} represses enzymes linked to nucleotide recycling, and triggers overexpression of proteases and enzymes linked to amino acids metabolism.

INTRODUCTION

Deinococcus radiodurans is a Gram-positive bacterium, belonging to the Deinococcales order, whose members feature outstanding resistance to DNA-damaging agents [1]. Indeed, after its isolation from canned meat samples exposed to γ rays [2], *D. radiodurans* was the subject of quite a number of studies dealing with the competence of this bacterium in withstanding exposure to ionizing radiations. Early work was devoted to the investigation of the biochemical mechanisms exerted by *D. radiodurans* to repair damaged DNA [3-10]. Rather surprisingly, cells of *D. radiodurans* exposed to 14 kGy, and containing fragmented chromosomes, are able to reassemble their genomes within 6-7 h after radiation exposure [1]. Contrary to the vast majority of prokaryotes, *D. radiodurans* cells are polyploid, with the actual ploidy number being affected by growth phase [11] and culture medium [12]. Each genome copy consists of two chromosomes (containing 2.6 and 0.4 Mbp) and two plasmids, featuring $177 \bullet 10^3$ and $45.7 \bullet 10^3$ bp, respectively [13]. When this complex genome undergoes fragmentation, the essential 5'-3' exonuclease RecJ [14] produces 3' overhangs at the chromosomal/plasmid fragments, inducing the RecFOR-mediated loading of RecA onto DNA. The concerted action of RecA and DNA Polymerase DnaE recombine and extend the overlapping homologous fragments [15], according to a mechanism denoted ESDSA (Extensive Synthesis-Dependent Strand Annealing). While polyploidy is an obvious requisite for genome reconstruction competence, *D. radiodurans* does also feature additional and peculiar biochemical properties, responsible for genome integrity maintenance. Considering that ionizing radiations induce severe oxidative stress, it was realized that the radiation-resistance of *D. radiodurans* is mainly due to biochemical factors preserving the proteome of this bacterium from oxidation damages [1]. Among these biochemical factors, manganese is considered a relevant component, mainly because of the following observations: i) the cellular concentration of manganese in *D.*

radiodurans is high, ranging from 0.2 to 4 mM [16-18]; ii) *in vitro*, Mn^{2+}, in complex with phosphate ions, peptides, or amino acids, catalyzes the scavenging of superoxide radical [19, 20] and hydrogen peroxide [21]; iii) the depletion of Mn^{2+} from the culture medium triggers oxidative stress in *D. radiodurans* [22]. Therefore, it is not surprising that Mn^{2+} represents one of the main determinants of *D. radiodurans* ability to survive ionizing radiations. Remarkably, it was shown that the addition of 2.5 µM Mn^{2+} to solid medium was necessary for the growth of *D. radiodurans* cells in Petri dishes exposed to 50 Gy/hour [17]. In addition, it was also shown that a positive correlation exists between the level of radioresistance and the intracellular Mn/Fe molar ratio observed in different bacteria [17]. It should however be noted that the addition of Mn^{2+} to the growth medium is not necessarily beneficial to *Deinococcus radiodurans*. It was indeed shown that Mn^{2+} can induce a futile Embden-Meyerhof-Parnas pathway, and decreases the survival of *D. radiodurans* to UV light [23]. Moreover, the addition of Mn^{2+} to liquid cultures of *D. radiodurans* at early stationary phase triggers, in comparison with control cultures, an increase of biomass first, and a subsequent and pronounced decrease of live individuals in the bacterial population [24].

While the information relative to the protective role of manganese against ionizing radiations and oxidative damage is quite consistent, the effects that this metal can exert *per se* on the growth of *D. radiodurans* are poorly characterized. Early enough, it was recognized, and subsequently confirmed, that Mn^{2+} added to liquid cultures in rich medium at early stationary phase induces about 3 additional cell cycles and doubles the biomass yield [23-25]. Similar observations were reported for *Deinococcus geothermalis* [26]. Recently, the addition of Mn^{2+} to cultures of *D. radiodurans* at logarithmic phase in rich liquid medium was reported to increase biomass yield, although it did not affect the growth rate [27]. However, it was also reported that the addition of 5 µM Mn^{2+} to rich liquid medium decreased the growth rate of *D. radiodurans* [28], and that the effect of Mn^{2+} on the biomass yield is lower when compared with

the increase in population density triggered by Mg^{2+}, under optimal growth conditions [22]. Nevertheless, it was demonstrated that Mn^{2+} is essential for *D. radiodurans* growth. Indeed, no significant growth was observed in a defined minimal medium (DMM) in the absence of Mn^{2+} [17]. Moreover, it was shown that supplementing the medium with Mn^{2+} in the 0.25-500 nM concentration interval did progressively increase both the growth rate and the biomass yield [17]. No further effects were observed when the divalent cation was present at concentrations higher than 500 nM.

A detailed study of the *D. radiodurans* growth kinetics as affected by the addition of Mn^{2+} to TGY (Tryptone, Glucose, Yeast extract) rich medium is presented here, along with a parallel comparison of the proteomes of cells collected at late logarithmic and stationary phase, and grown in standard or Mn^{2+}-enriched TGY medium. The observations accordingly obtained are discussed, taking into account the intracellular Mn^{2+} levels, experimentally determined in the different *D. radiodurans* populations considered.

MATERIALS AND METHODS

Strain and growth medium

Deinococcus radiodurans DSM 46620 was obtained from the Deutsche Sammlung von Mikroorganismen und Zellkulturen (DSMZ, Braunschweig, Germany), and grown in TGY medium (Tryptone, Glucose, and Yeast extract at 5, 1, and 3 g/L, respectively) at 30 °C under constant shaking (200 rpm).

Determination of growth in liquid media

The growth of *D. radiodurans* DSM 46620 in TGY liquid medium, supplemented or not with $MnCl_2$, was evaluated spectroscopically, and by cell and colony counting. Aliquots withdrawn from liquid cultures as a function of time were used to determine their Absorbance at 600 nm. In addition, the same aliquots were used for cell and colony counting, by means of a Thoma chamber (depth 5 µm, Poly-Optik GmbH, Blankenburg, Germany) and TGY solid medium, respectively.

Microscopy

From Petri dishes, 2 isolated colonies were used to obtain 2 independent pre-cultures in TGY medium at 30 °C. Each pre-culture was used after 24 h to inoculate 2 flasks containing 25 mL of TGY each. Morphology of cells from cultures incubated in TGY medium containing 0, 5, 25 or 250 µM $MnCl_2$ was evaluated 0, 12, 15 and 25 hours after dilution. Intracellular levels of Mn^{2+} were revealed using a turn-on BODIPY-based fluorescent probe, the selectivity of which was previously described [29]. From cultures incubated in TGY medium containing 0, 5, 25, or 250 µM $MnCl_2$, a 1mL aliquot was taken and washed 3 times with TBS to remove the excess of $MnCl_2$ of the medium. The BODIPY-based Mn^{2+} sensor (70 µM) was added to each sample and incubated at 30 °C for 15 minutes. Samples were washed 3 times with PBS and imaged with a

Nikon Eclipse T1 microscope (Nikon Plan Fluor × 100/1.30 Oil Ph3 DLL objective) coupled to an EMCCD camera. Images were analyzed using ImageJ software [30].

Sample preparation for 2D-PAGE

In order to remove lipids and carotenoids from the more external layers, frozen cells from 25 mL of cultures were incubated with absolute ethanol for 15 minutes on ice. Cells suspensions were then centrifuged at 16,000 g for 10 minutes and pellets were resuspended in 0.5 mL of lysis buffer (7 M Urea, 2 M Thiourea, 4% w/v CHAPS, 50 mM DTT, 1 mM Sodium EDTA, 20 mM Tris base, IPG buffer 3-10, pH 6.8), containing Protease Inhibitors Cocktail (GE Healthcare, Piscataway, USA). Cells were sonicated for 2.5 minutes (cycles of 15 seconds with 1 minute intervals) on ice using a Branson Digital Sonifier (Thermo Fisher Scientific, Waltham, USA) at 20 % of amplitude, and then centrifuged for 20 minutes at 16,000 g to pellet insoluble components. Supernatants were collected, and protein concentration was determined using the Bradford Quick Start™ reagent (BioRad, Hercules, USA). Then, about 500 µg of total proteins from each sample were purified by ReadyPrep 2D Clean Up kit (BioRad), according to manufacturer's instructions, and precipitated proteins were resuspended in lysis buffer. The protein concentration of purified samples was determined as above, and aliquots were stored at -80°C.

2D Electrophoresis

For each sample, a 190 µg of total protein was diluted to 250 µl with rehydration solution, containing 7 M Urea, 2 M Thiourea, 4 % CHAPS, 0.5 % IPG buffer 4-7 (GE Healthcare), 1.2 % DeStreak™ reagent (GE Healthcare) and Bromophenol Blue in trace amount. Immobiline Dry Strips gels (pH 4-7, 11 cm, GE Healthcare) were passively rehydrated overnight in strip holders and electrofocused in Ettan IPGphor 3 (GE Healthcare). Focusing (20000 V•hrs) was carried out at 50 µA/strip and 15 °C, 500 V (5 h), 1000 V (2 h), gradient to 8000 V, 8000 V to end. IPG strips were incubated for 15 minutes in equilibration buffer (6 M Urea, 30 % v/v glycerol, 2 %

w/v SDS, 75 mM Tris HCl buffer, pH 8.8) containing 130 mM DTT, and then for further 15 minutes in equilibration buffer containing 135 mM Iodoacetamide. Strips were sealed in place on top of Criterion Precasted Gels–Any kD (BioRad) using 1 % w/v agarose in running buffer with trace amount of bromophenol blue. The second dimension was performed using a Criterion electrophoresis cell (BioRad) under constant current (30 mA/gel and 250 V max). Gels were fixed in 40 % v/v Methanol and 10 % v/v Acetic Acid solution for 2 hours, and then stained overnight with Colloidal Coomassie Blue G solution. After several washes, gels were scanned with Pharos-FX system and analyzed using Proteomweaver™ software (both from BioRad).

Preparation of samples for mass spectrometry

Spots were excised from gels and treated as reported by Shevchenko et al. [31]. Briefly, spots were destained in 50 mM ammonium bicarbonate in acetonitrile (ACN) and dehydrated with pure ACN. Samples were then reduced with 10 mM DTT, and alkylated with 55 mM iodoacetamide in 100 mM ammonium bicarbonate (Millipore-Sigma, St. Louis, USA). After dehydration in ACN, gel pieces were equilibrated at 4 °C in solution A (10 mM ammonium bicarbonate, 10 % ACN) containing 13 ng/µl of porcine trypsin for MS (Millipore-Sigma) for 2 hours, and then incubated at 37 °C overnight. After spinning, supernatants were harvested and gel pieces were covered by extraction solution (5 % formic acid in ACN). After 15 minutes of incubation at 37 °C, supernatants from this step where pooled to the corresponding supernatants of the previous step and dried in SpeedVac (Savant™).

Mass spectrometry

Separation of peptides were performed as previously described [32]. The resulting peptides were analyzed by LC-MS/MS using an Orbitrap XL instrument (Thermo Fisher Scientific) equipped with a nano-ESI source coupled with a nano-Acquity capillary UPLC (Waters, Milford, USA). Briefly, peptides were separated with a capillary BEH C18 column (0.075 x 100 mm, 1.7

169 μM, Waters) using aqueous 0.1 % formic acid (A) and CH_3CN containing 0.1 % formic acid (B)
170 as mobile phases. Peptides were eluted by means of a linear gradient from 5 to 50 % of B in 90
171 minutes, at a 300 nL/minute flow rate. Mass spectra were acquired over an *m/z* range from 400
172 to 1800. To achieve protein identification, MS and MS/MS data underwent Mascot Search
173 Engine software analysis to interrogate the National Center for Biotechnology Information non
174 redundant (NCBInr) protein database. Parameters sets were: trypsin cleavage;
175 carbamidomethylation of cysteines as a fixed modification, and methionine oxidation as a
176 variable modification; a maximum of two missed cleavages; false discovery rate, calculated by
177 searching the decoy database, was set at 0.05.

178 ***Atomic absorption spectroscopy***

179 The concentration of Mn^{2+} in liquid samples was determined using a Varian Spectra AA•100
180 GTA110 Spectrometer, equipped with a graphite furnace. The calibration curve was obtained
181 by dilution of a commercial standard (1000 ppm, Carlo Erba, Cornaredo, Italy) to 20, 40, 60,
182 and 80 ppb. For the analysis of glucose, tryptone and yeast extract, 1 g of each sample was
183 individually dissolved in 24.75 mL of ultrapure H_2O to which 250 μL of HNO_3 was added. The
184 solutions accordingly obtained were then analyzed. For the estimation of Mn^{2+} in *D.*
185 *radiodurans* cells, aliquots of liquid cultures (1 mL) were centrifuged and the resultant pellets
186 were washed twice with ultrapure H_2O. Finally, the washed pellets were resuspended and
187 subjected to analysis.

188

189

190

RESULTS AND DISCUSSION

Growth of Deinococcus radiodurans in TGY medium enriched with Mn^{2+}

As a first test, we assayed the growth of *Deinococcus radiodurans* at 30 °C in TGY medium to which 0, 2.5, 5, 10, 25, or 250 μM Mn^{2+} was added. Accordingly, we spectroscopically determined the growth kinetics of the corresponding bacterial populations, of which the majority did reach the stationary phase within 35 h (Fig. 1a). The addition of Mn^{2+} to the medium positively affected the biomass yield, and at concentrations ≥ 10 μM increased the time length of the lag phase. In particular, when compared to the control, all the cultures grown in manganese-enriched TGY medium featured a higher population density at the end of the time interval considered (Fig. 1a). When the lag phase is analyzed, 10, 25 and 250 μM Mn^{2+} did significantly delay the onset of growth, by about 10, 15, and 20 h, respectively (Fig. 1a). In contrast, the addition of 2.5 or 5 μM manganese to TGY medium did neither alter the lag phase nor the growth rate, but increased the biomass yield about 1.5 fold when compared to the control culture (Fig. 1a). We further tested this effect by comparing control and manganese-supplemented cultures. To this aim, 3 single colonies of *D. radiodurans* were used to inoculate 3 independent pre-cultures, whose growth was performed in TGY medium at 30 °C for 48 h. Each pre-culture was then diluted in TGY and in the same medium to which 5 μM Mn^{2+} was added, and the 6 cultures accordingly obtained were incubated for 15 h at 30 °C, under constant shaking. Based on the determined growth kinetics of each culture, we observed significant higher biomass yields in the manganese-supplemented cultures (Supplementary Fig. S1). To better define the stimulation of *D. radiodurans* growth exerted by Mn^{2+}, the biomass yield by cell and colony counting, after 19 h of growth at 30 °C, was estimated. When the number of individuals per unit volume was determined using a Thoma chamber, we observed that the addition of Mn^{2+} doubled the population density (Fig. 1b). A similar magnitude of the effect

induced by manganese was also observed by colony counting (Fig. 1b). Not surprisingly, the absolute values were in this case slightly lower than those relative to the number of total cells per unit volume, for both the control and the manganese-supplemented cultures. It is important to note that the addition of manganese to TGY medium, besides inducing a significant increase in biomass yield (Fig. 1b), did not dramatically affect the partition of the bacterial population among single cells, diads, and tetrads (Fig. 2). The only significant effect observed was indeed a slight increase of the occurrence of diads and tetrads in the population grown in manganese-supplemented medium (Fig. 2).

The formulation of a defined minimal medium (DMM) for *Deinococcus radiodurans* [33] was a mandatory step to recognize manganese as essential for the growth of this microorganism [17]. The effect on *D. radiodurans* growth eventually induced by the addition of manganese to rich media was tested under different conditions. Generally, high concentrations (100-500 μM) of $MnCl_2$ were chosen to inoculate a TGY-enriched medium [24, 28], or to supplement TGY at stationary [23-25] or logarithmic phase [27]. Nevertheless, Chou and Tan observed that concentrations of Mn^{2+} in the 0-2.5 μM interval suffice to increase the biomass yield of *D. radiodurans* in rich medium [24]. Overall, these observations agree in suggesting that the concentration of manganese in rich media is sub-optimal when the biomass yield is considered. Despite this agreement, conflicting evidence was reported about the effect of Mn^{2+} towards the growth kinetics of *D. radiodurans* in rich media. The divalent cation was indeed shown to be ineffective [23, 27] or detrimental [23, 25, 28] towards the growth rate. We reported here that concentrations of $MnCl_2$ ranging from 2.5 to 250 μM did not significantly alter the growth rate of *D. radiodurans*, albeit triggering higher biomass yields (Fig. 1a). However, we observed a consistent increase of the time length of the lag phase as the TGY medium was supplemented with manganese at concentrations higher than 10 μM (Fig. 1a). The divergence between our and previous observations is quite likely due to the method we used to prepare the cultures:

contrary to what customarily done [23, 28], we did not pre-culture cells in manganese-enriched medium, but we instead used a single pre-culture grown in TGY medium, and this single pre-culture was subsequently split in 2 cultures, in TGY and in TGY supplemented with $MnCl_2$, respectively. This means, in turn, that the cells we grew in TGY Mn^{2+}-enriched medium were adapting to the presence of the divalent cation, most likely by expressing proteins useful to deal with the presence of manganese. In our view, this was important to obtain meaningful samples for protein extraction and mass spectrometry, with the aim to identify components of the proteome responsible for the positive response of *D. radiodurans* to manganese.

Mn^{2+} levels in *Deinococcus radiodurans* cells

To evaluate the propensity of *D. radiodurans* cells to accumulate Mn^{2+}, we analyzed by atomic absorption spectroscopy the concentration of this divalent cation both in TGY medium and in whole cells. First, we determined the concentration of Mn^{2+} in the 3 components of TGY, *i.e.* tryptone, yeast extract, and glucose. Using solutions at 40 g/L of each compound, we were able to determine 3.05 ± 0.09, and 2.19 ± 0.08 µg/g (ppb) of Mn^{2+} in tryptone and yeast extract, respectively. The content of the divalent cation in glucose was below the detection limit of our procedure, equal to 0.4 µg/g. Accordingly, and considering the composition of TGY (Tryptone, Glucose, and Yeast Extract at 5, 1, and 3 g/L, respectively), the concentration of Mn^{2+} in the medium was equal to 21.82 µg/L, *i.e.* 0.4 µM. The manganese concentration was then determined in whole cells grown for 15 or 19 h in TGY, or in the same medium to which 5 µM Mn^{2+} was added. To estimate the manganese concentration *in vivo*, the number of cells of each sample was counted with a Thoma chamber, and the volume of a single cell was assumed as equal to 8 μm^3. According to this assumption, the data obtained for cells cultured for 15 h (Supplementary Fig. S2a) correspond to 0.2 and 0.75 mM of Mn^{2+} per single cell, grown in TGY or in manganese-supplemented medium, respectively. For cells grown for 19 h, this difference does hold, the Mn^{2+} concentration being indeed equal to 0.5 and 1.45 mM for cells grown in

266 control and in manganese-supplemented medium, respectively (Supplementary Fig. S2b).
267 Accordingly, the addition of 5 μM $MnCl_2$ to TGY induces a 3-fold increase of Mn^{2+} concentration
268 *in vivo*, independently of the growth phase. This suggests that the enrichment of TGY with $MnCl_2$
269 should induce significant changes in *D. radiodurans* proteome at early stages of growth.
270 Considering the effect exerted by Mn^{2+} on cell growth, we also evaluated whether Mn^{2+} addition
271 to the medium affects the cell morphology. Among the comparisons considered, some
272 significant differences were observed (Table 1): i) at 12 h of incubation or later, the cells axes
273 of control cells were longer than those of cells grown in the presence of manganese; ii) at 20-
274 25 h of incubation, cells incubated in the presence of 250 μM manganese featured shorter axes;
275 iii) the addition of 25 or 250 μM manganese shortened the diameter of cells incubated for 12
276 or 20 h, and this effect lasted for 25 h of incubation for cells grown in the presence of 250 μM
277 manganese. The peculiar morphology of control cells does nicely correlate with the observation
278 that the growth of these cells slows down after 15 h of incubation (Fig. 1a), suggesting a
279 phenotypic link between the elongation of cells axis and the onset of stationary phase. In
280 addition, we observed a significant shortening of cells diameter in those populations featuring
281 a prolonged lag phase (Table 1, Fig. 1a). It is also important to note that no aberrant
282 morphologies were observed for any of the concentrations of Mn^{2+} tested (Fig. 3a).
283 We also determined in another experiment the cytosolic accumulation of Mn^{2+} in cells cultured
284 in the absence (control) or in the presence (5, 25 or 250 μM) of $MnCl_2$, under the same growth
285 conditions. To this aim, we used a BODIPY-based turn-on fluorescent Mn^{2+} sensor, which can
286 pass the cell membrane and bind specifically to intracellular Mn^{2+} [29]. Cells grown in the
287 absence of $MnCl_2$ show a total fluorescence equal to 45.82 ± 20.64. This signal increases 3.2
288 (146.97 ± 68.40), 3.64 (166.97 ± 85.02) and 4.91 (225.02 ± 71.69) times for the samples grown
289 in the presence of 5, 25 and 250 μM $MnCl_2$, respectively (Fig.s 3b and 3c). However, the only
290 significant difference among those detected is the divergence between the total fluorescence of

291 cells grown in the absence of manganese and the fluorescence levels of cells grown in
292 manganese-enriched media (Fig. 3c). This could be due to the following reasons: i) the probe
293 concentration is limiting; ii) most of the Mn^{2+} is bound to proteins and DNA, and therefore is
294 not accessible to the probe. In addition, we observed that at high Mn^{2+} enrichment (250 μM) of
295 the growth medium, the cytosolic probe bleached faster than the membrane bound.

296 ***Mn^{2+} and the proteome of Deinococcus radiodurans***

297 Taking into account the growth-promoting effect induced in *D. radiodurans* by manganese (Fig.
298 1), and the concomitant accumulation *in vivo* of this divalent cation (Fig. 3), we investigated in
299 detail the proteome of cells grown in TGY or in the same medium enriched with 5 μM Mn^{2+}.
300 Considering the kinetics of growth in both media (Fig. 1a), we decided to harvest cells from
301 cultures grown for 15 and 19 h. By this means, we compared the proteome of control and
302 manganese-enriched cells when their growth phase was comparable (15 h, Fig. 1a) and when
303 the difference in population density between the 2 cultures was well established (19 h, Fig. 1a).
304 From each sample total proteins were extracted to perform 2D electrophoresis, and the spot
305 patterns of the 4 gels were compared. A total of 68 spots that were absent or overexpressed
306 (spots whose intensity was at least 2-fold higher or lower than the matched spot on the other
307 gel) in the control or in the Mn^{2+}-treated culture were selected for MS analysis. The complete
308 list of the proteins associated to these spots is reported in Supplementary Table ST1, where it
309 is shown that some proteins could not be identified, and others were identified as sample
310 contaminants (e.g. keratin in spot 19, Supplementary Table ST1). In addition, some spots were
311 found to contain *D. radiodurans* proteins whose function is hypothetical. Excluding from further
312 analysis the proteins not identified, and those representing contaminants or featuring
313 hypothetical functions, a total of 52 spots was left for the comparison of the 4 proteomes
314 considered.

315 Interestingly, among these spots we observed 5 whose electrophoretic mobility was
316 significantly affected by the enrichment with manganese of the growth medium (Table 2, Fig.s
317 4 and 5). These 5 proteins isolated from manganese-enriched cultures featured higher pI
318 values, with shifts up to 1.4 pH units (Table 2). It is important to note that the most consistent
319 pI shift (1.4) is associated to an iron ABC transporter, the molecular mass of which was found
320 almost invariant (Table 2). The regulation of ABC transporters by phosphorylation is well
321 documented [34], and the importance of kinases as well as the presence of phosphorylation
322 sites has been reported [35-37]. Accordingly, we propose that in cells grown in Mn^{2+}-enriched
323 medium the extent of phosphorylation of the iron ABC transporter is significantly reduced
324 when compared to that at the expense of the protein from control cells, leading to a higher pI.
325 This would, in turn, lead to a decreased activity of the iron transporter in manganese-enriched
326 cells. It was previously shown that the radio-resistance of *D. radiodurans* is correlated to high
327 manganese/iron ratio, *in vivo* [17]. Accordingly, the behaviour reported here for the iron ABC
328 transporter suggests a mechanism for the beneficial effect exerted by Mn^{2+} under physiological
329 growth conditions. In addition, the observations listed in Table 2 suggest to attempt, with
330 future work, the identification of post-translational modification systems affected by
331 manganese.
332 When the proteomes of control and manganese-enriched cells were compared after 15 h of
333 growth, we detected 7 and 9 proteins preferentially expressed in control (Supplementary Table
334 ST2, Fig. 4) and in manganese-enriched (Supplementary Table ST3, Fig. 4) cells, respectively.
335 Furthermore, by comparing the two proteomes after 19 h of growth, we identified 9 and 21
336 proteins selectively expressed in control (Supplementary Table ST4, Fig. 5) and in manganese-
337 enriched (Supplementary Table ST5, Fig. 5) cells, respectively. The 46 proteins accordingly
338 identified can be classified into 4 major groups: i) the extracellular nuclease (Gi10957459) and
339 the ribosomal 50S L5 protein (Gi15805352) are exclusively expressed in control cells, both

after 15 and 19 h of growth (spots 1 and 11, 2 and 13, Supplementary Tables ST2 and ST4); ii) the transcription termination/anti-termination factor NusA (Gi15806798) is selectively expressed in manganese-enriched cells, both after 15 and 19 h of growth (spots 10 and 24, Supplementary Tables ST3 and ST5); iii) the phage shock protein A (Gi15806486) is earlier expressed in control cells (spots 4 and 63, Supplementary Tables ST2 and ST5); the V-type ATPase subunit A (Gi15805727) is earlier expressed in manganese-enriched cells (spots 31 and 40, Supplementary Tables ST3 and ST4); iv) the remaining 38 proteins were peculiar of both the medium and the growth phase (i.e. expressed in one medium only, at 15 or 19 h of growth). Concerning the extracellular nuclease, its selective expression in control cells suggests that this enzyme sustains the recycling of nucleotides from DNA exported into the growth medium after oxidative damage, whose occurrence could be prevented by Mn^{2+}. This suggestion is sustained by the observation that purine nucleoside phosphorylase, a well-known phosphate-dependent component of the purine salvage pathway [38, 39], is also selectively expressed in control cells (Supplementary Table ST2). To this, it could be related the concomitant selective expression in control cells of the phosphate ABC transporter (Supplementary Table ST2). The exclusive detection (Supplementary Tables ST2 and ST3) and the overexpression (Supplementary Tables ST4 and ST5) of NusA in manganese-enriched cells can be related to the higher biomass yield triggered by Mn^{2+} addition to TGY medium. Remarkably, the rate of synthesis of NusA was quantified in *Escherichia coli* as a function of medium composition, and it was shown that the expression of this transcriptional regulator is increased five-fold in cells grown in rich medium, when compared to the level detected in cells grown in minimal medium [40]. The ribosomal proteins reported in Supplementary Tables ST2-ST5 deserve a detailed comment. *D. radiodurans* is known to contain 3 ribosomal operons [41], featuring low diversity among the 23S rRNA genes. Despite this redundancy at the genomic level, our proteomic data reported in Supplementary Tables ST2-ST5 could erroneously suggest that control or manganese-enriched

365 *D. radiodurans* cells are devoid of a particular ribosomal protein. On the contrary, it has to be
366 noted that: i) for ribosomal protein L1 a shift in pI was detected (Table 2); ii) for the same L1
367 protein we also detected an additional spot in control cells (Supplementary Table ST2), but this
368 spot does contain a truncated form of the L1 protein (25 kDa vs. the 30 kDa of full-length
369 protein); iii) the L5 ribosomal protein is apparently expressed only by control cells
370 (Supplementary Tables ST2 and ST4); it should however be remarked that the observed pI of
371 this protein was extremely lower (4.25) than the theoretical value (9.88); therefore, it is quite
372 likely that the L5 protein associated to these spots (2 and 13) represents a post-translationally
373 modified sub-population of the total amount of this ribosomal protein; iv) a particular situation
374 was observed for the 30S ribosomal S2 protein (Supplementary Table ST5): in this case, the
375 molecular mass of the protein detected in manganese-enriched cells was determined as higher
376 (37 kDa) than the expected value (30 kDa), therefore representing a pool of S2 protein
377 exclusively modified in manganese-enriched cells.
378 It should be noted that 15 h old cells represent individuals entering the stationary phase or
379 engaged in the logarithmic phase in the absence or in the presence of additional Mn^{2+},
380 respectively (Fig. 1a). Therefore, the proteins reported in Supplementary Table ST3 should be
381 diagnostic of the competence of manganese-enriched cells to sustain additional cell cycles
382 before reaching the stationary phase. In this frame, the identification of enzymes involved in
383 peptide and amino acids metabolism (Alanine-DH, Serine-OH methyl transferase, oligo
384 endopeptidase F) seems particularly meaningful when considering that *D. radiodurans* is a
385 proteolytic bacterium [1]. Moreover, the presence in this group of the molecular chaperone
386 DnaJ, which is known to assist DnaK in the hydrolysis of ATP [42], further suggests that *D.*
387 *radiodurans* cells grown for 15 h in Mn^{2+}-enriched medium are competent in sustaining
388 additional doublings. A similar situation does likely hold for cells collected after 19 h of growth,
389 which correspond to full stationary and late-logarithmic phase for control and manganese-

enriched cells, respectively (Fig. 1a). Among the proteins selectively detected in manganese-enriched cells, it is interesting to outline the presence of enzymes diagnostic of active metabolism and growth (S-protease, protease I, translation IF-2, N-acetyl-muramoyl-L-Ala amidase, Supplementary Table ST5). In addition, it should however be noted that among these proteins we detected enzymes involved in stress-responses (catalase, DNA-binding stress response) and in the regulation of ATP availability (adenylate kinase), diagnostic of the incoming stationary phase (Fig. 1a).

CONCLUDING REMARKS

We have shown here that under physiological conditions the addition of Mn^{2+} to the TGY rich medium stimulates the growth of *D. radiodurans*, and significantly alters the proteome of this bacterium. In particular, we observed that Mn^{2+} can affect both the expression level and the post-translational modification of proteins. Accordingly, future work will be devoted to identify these post-translational modifications and to characterize the phenotype of *D. radiodurans* strains bearing mutations at the expense of some of the proteins identified here.

Funding information

The work did not receive support from public or private Institutions.

Conflicts of interest

The authors declare that there are no conflicts of interest.

REFERENCES

1. Slade D, Radman M. Oxidative stress resistance in *Deinococcus radiodurans*. *Microbiol Mol Biol Rev* 2011;75:133-191.
2. Anderson AW, Nordan HC, Cain RF, Parrish G, Duggan D. Studies on a radio-resistant micrococcus. I. Isolation, morphology, cultural characteristics, and resistance to gamma radiation. *Food Technol* 1956;10:575-577.
3. Dean CJ, Feldschreiber P, Lett JT. Repair of X-ray damage to the deoxyribonucleic acid in *Micrococcus radiodurans*. *Nature* 1966;209:49-52.
4. Moseley BE. The isolation and some properties of radiation–sensitive mutants of *Micrococcus radiodurans*. *J Gen Microbiol* 1967;49:293-300.
5. Moseley BE. Repair of ultraviolet radiation damage in sensitive mutants of *Micrococcus radiodurans*. *J Bacteriol* 1969;97:647-652.
6. Driedger AA, James AP, Grayston MJ. Cell survival and X-ray-induced DNA degradation in *Micrococcus radiodurans*. *Radiat Res* 1970;44:835-845.
7. Burrell AD, Feldschreiber P, Dean CJ. DNA-membrane association and the repair of double breaks in X-irradiated *Micrococcus radiodurans*. *Biochim Biophys Acta* 1971;247:38-53.
8. Hariharan PV, Cerutti PA. Formation and repair of gamma-ray induced thymine damage in *Micrococcus radiodurans*. *J Mol Biol* 1972;66:65-81.
9. Bonura T, Bruce AK. The repair of single-strand breaks in a radiosensitive mutant of *Micrococcus radiodurans*. *Radiat Res* 1974;57:260-275.
10. Sweet DM, Moseley BE. The resistance of *Micrococcus radiodurans* to killing and mutation by agents which damage DNA. *Mutat Res* 1976;34:175-186.

11. Hansen MT. Multiplicity of genome equivalents in the radiation-resistant bacterium *Micrococcus radiodurans*. *J Bacteriol* 1978;134:71-75.

12. Harsojo, Kitayama S, Matsuyama A. Genome multiplicity and radiation resistance in *Micrococcus radiodurans*. *J Biochem* 1981;90:877-880.

13. White O, Eisen JA, Heidelberg JF, Hickey EK, Peterson JD *et al.* Genome sequence of the radioresistant bacterium *Deinococcus radiodurans* R1. *Science* 1999;286:1571-1577.

14. Moseley BE, Mattingly A, Shimmin M. Isolation and some properties of temperature-sensitive mutants of *Micrococcus radiodurans* defective in DNA synthesis. *J Gen Microbiol* 1972;70:399-409.

15. Zharadka K, Slade D, Bailone A, Sommer S, Averbeck D *et al.* Reassembly of shattered chromosomes in *Deinococcus radiodurans*. *Nature* 2006;443:569-573.

16. Leibowitz PJ, Schwartzberg LS, Bruce AK. The in vivo association of manganese with the chromosome of *Micrococcus radiodurans*. *Photochem Photobiol* 1976;23:45-50.

17. Daly MJ, Gaidamakova EK, Matrosova VY, Vasilenko A, Zhai M *et al.* Accumulation of Mn(II) in *Deinococcus radiodurans* facilitates gamma-radiation resistance. *Science* 2004;306:1025-1028.

18. Daly MJ, Gaidamakova EK, Matrosova VY, Vasilenko A, Zhai M *et al.* Protein oxidation implicated as the primary determinant of bacterial radioresistance. *PLoS Biol* 2007;5:e92.

19. Archibald FS, Fridovich I. The scavenging of superoxide radical by manganous complexes: in vitro. *Arch Biochem Biophys* 1982;214:452-463.

20. Barnese K, Gralla EB, Cabelli DE, Valentine JS. Manganous phosphate acts as a superoxide dismutase. *J Am Chem Soc* 2008;130:4604-4606.

21. Berlett BS, Chock PB, Yim MB, Stadtman ER. Manganese(II) catalyzes the bicarbonate-dependent oxidation of amino acids by hydrogen peroxide and the amino acid-facilitated dismutation of hydrogen peroxide. *Proc Natl Acad Sci USA* 1990;87:389-393.

22. He Y. High cell density production of *Deinococcus radiodurans* under optimized conditions. *J Ind Microbiol Biotechnol* 2009;36:539-546.

23. Zhang YM, Wong TY, Chen LY, Lin CS, Liu JK. Induction of a futile Embden-Meyerhof-Parnas pathway in *Deinococcus radiodurans* by Mn: possible role of the pentose phosphate pathway in cell survival. *Appl Env Microbiol* 2000;66:105-122.

24. Chou FI, Tan ST. Manganese(II) induces cell division and increases in superoxide dismutase and catalase activities in an aging Deinococcal culture. *J Bacteriol* 1990;172:2029-2035.

25. Lee H, Wong T, Kuo J, Liu J. The effect of Mn(II) on the autoinducing growth inhibition factor in *Deinococcus radiodurans*. *Prep Biochem Biotechnol* 2014;44:645-652.

26. Liedert C, Peltola M, Bernhardt J, Neubauer P, Salkinoja-Salonen M. Physiology of resistant *Deinococcus geothermalis* bacterium aerobically cultivated in low-manganese medium. *J Bacteriol* 2012;194:1552-1562.

27. Santos SP, Mitchell EP, Franquelim HG, Castanho MARB, Abreu IA *et al.* Dps from *Deinococcus radiodurans*: oligomeric forms of Dps1 with distinct cellular functions and Dps2 involved in metal storage. *FEBS J* 2015;282:4307-4327.

28. Holland AD, Rothfuss HM, Lidstrom ME. Development of a defined medium supporting rapid growth for *Deinococcus radiodurans* and analysis of metabolic capacities. *Appl Microbiol Biotechnol* 2006;72:1074-1082.

29. Bakthavatsalam S, Sarkar A, Rakshit A, Jain S, Kumar A *et al.* Tuning macrocycles to design 'turn on' fluorescence probes for manganese(II) sensing in live cells. *Chem Comm* 2015;51:2605-2608.

30. Vischer NOE, Verheul J, Postma M, van den Berg van Saparoea B, Galli E *et al.* Cell age dependent concentration of *Escherichia coli* divisome proteins analyzed with ImageJ and ObjectJ. *Front Microbiol* 2015;6:586.

31. Shevchenko A, Tomas H, Havliš J, Olsen JV, Mann M. In-gel digestion for mass spectrometric characterization of proteins and proteomes. *Nat Protoc* 2007;1:2856-2860.

32. Conte E, Vincelli G, Schaaper RM, Bressanin D, Stefan A *et al.* Stabilization of the *Escherichia coli* DNA polymerase III ε subunit by the θ subunit favors *in vivo* assembly of the Pol III catalytic core. *Arch Biochem Biophys* 2012;523:135-143.

33. Venkateswaran A, McFarlan SC, Ghosal D, Minton KW, Vasilenko A *et al.* Physiologic determinants of radiation resistance in *Deinococcus radiodurans*. *Appl Environ Microbiol* 2000;66:2620-2666.

34. Stolarczyk EI, Reiling CJ, Paumi CM. Regulation of ABC transporter function via phosphorylation by protein kinases. *Curr Pharm Biotechnol* 2011;12:621-635.

35. Mayati A, Moreau A, Le Vée M, Stieger B, Denizot C *et al.* Protein kinases C-mediated regulations of drug transporter activity, localization and expression. *Int J Mol Sci* 2017;18:764.

36. Anreddy N, Gupta P, Kathawala RJ, Patel A, Wurpel JND *et al.* Tyrosine kinase inhibitors as reversal agents for ABC transporter mediated drug resistance. *Molecules* 2014;19:13848-13877.

37. Cohen P. The role of protein phosphorylation in human health and disease. The Sir Hans Krebs medal lecture. *Eur J Biochem* 2001;268:5001-5010.

38. Murray AW. The biological significance of purine salvage. *Ann Rev Biochem* 1971;40:811-826.

39. Bzowska A, Kulikowska E, Shugar D. Purine nucleoside phosphorylases: properties, functions, and clinical aspects. *Pharmacol Ther* 2000;88:349-425.

40. Li GW, Burkhardt D, Gross C, Weissman JS. Quantifying absolute protein synthesis rates reveals principles underlying allocation of cellular resources. *Cell* 2014;157:624-635.

41. Pei A, Nossa CW, Chokshi P, Blaser MJ, Yang L *et al.* Diversity of 23S rRNA genes within individual prokaryotic genomes. *PLos ONE* 2009;4:e5437.

42. Dekker SL, Kampinga HH, Bergink S. DNAJs: more than substrate delivery to HSPA. *Front Mol Biosci* 2015;2:35.

519 **FIGURE LEGENDS**

520 **Figure 1**

521 Manganese and growth of *Deinococcus radiodurans*. **(a)** Growth kinetics of *D. radiodurans*
522 in TGY liquid medium (green circles) or in the same medium supplemented with 2.5, 5, 10,
523 25, or 250 µM $MnCl_2$ (blue, red, purple, dark green, and cyano circles, respectively). **(b)**
524 Population density of *D. radiodurans* cultures grown for 19 h in TGY medium (red bars) or
525 in the same medium to which 5 µM $MnCl_2$ was added (green bars), as determined
526 spectroscopically (Absorbance at 600 nm), using a Thoma chamber (Individuals/mL) or by
527 colony counting (c.f.u./mL). Diads and tetrads were considered as single individuals. The
528 error bars represent standard deviation (n = 3). The experimental mean values were
529 compared by the Student's t test (**, ***, and **** indicate $P < 0.01$, <0.001, <0.0001,
530 respectively).

531

532 **Figure 2**

533 Distribution of *Deinococcus radiodurans* populations among single cells, diads, and tetrads.
534 Cultures of *D. radiodurans* were grown for 19 h in TGY medium (dark green bars) or in the
535 same medium supplemented with 5 µM $MnCl_2$ (green bars), and aliquots were withdrawn
536 for direct counting with a Thoma chamber. About 300 individuals were considered for each
537 sample, and the analysis was repeated in triplicate. Error bars represent standard deviation
538 (n = 3). The experimental mean values were compared by the Student's t test (* indicates P
539 < 0.05).

540

541 **Figure 3**

542 Phenotypes of *Deinococcus radiodurans* cells grown in TGY medium supplemented or not
543 with $MnCl_2$. **(a)** Representative cells of *D. radiodurans* cells grown at 30 °C in TGY medium,

to which 0 (control), 5, 25 or 250 μM $MnCl_2$ was added; samples were harvested 0, 12, 20 and 25 hours after pre-cultures dilution (for a morphological analysis see Table 1). **(b)** Phase contrast and fluorescence images of *D. radiodurans* cells incubated with a BODIPY-based Mn^{2+} sensor. **(c)** Total Fluorescence determined in *D. radiodurans* cells as a result of the accumulation of a BODIPY-based Mn^{2+} sensor that specifically binds intracellular Mn^{2+}. Number of cells analyzed was 895, 1012, 622, and 235 for the control, 5, 25, and 250 μM $MnCl_2$, respectively. Scale bar equals 2 μm. The experimental mean values were compared by the Student's t test (*** indicates $P < 0.001$).

Figure 4

Manganese and the proteome of *Deinococcus radiodurans.* 2D electrophoresis of protein extracts isolated from *D. radiodurans* cells grown for 15 h in TGY medium (**a**) or in the same medium supplemented with 5 μM $MnCl_2$ (**b**). The molecular mass in kDa of the markers used for the second dimension is reported on the left.

Figure 5

Manganese and the proteome of *Deinococcus radiodurans.* 2D electrophoresis of protein extracts isolated from *D. radiodurans* cells grown for 19 h in TGY medium (**a**) or in the same medium supplemented with 5 μM $MnCl_2$ (**b**). The molecular mass in kDa of the markers used for the second dimension is reported on the left.

Supplementary Figure S1

Manganese and growth of *Deinococcus radiodurans*. Growth kinetics of *D. radiodurans* in TGY liquid medium (green circles, squares, and triangles) or in the same medium supplemented with 5 μM $MnCl_2$ (blue circles, squares, and triangles). The growth kinetics

was determined for 3 independent cultures (3 different single colonies were used) of each sample (green symbols: TGY medium; blue symbols: TGY medium supplemented with 5 μM $MnCl_2$). The horizontal bars represent the mean of the final Absorbance values determined for the two groups of cultures (the error bars indicate standard deviation). The experimental mean values were compared by the Student's t test (*** indicates $P < 0.001$).

Supplementary Figure S2

Manganese levels in cells of *Deinococcus radiodurans*. Cultures of *D. radiodurans* were grown for 15 and 19 h (Panels a and b, respectively) in TGY medium, or in the same medium supplemented with 5 μM $MnCl_2$. The content of Mn^{2+} in whole cells grown in TGY (green squares) or in medium supplemented with 5 μM $MnCl_2$ (blue squares) was determined by atomic absorption spectroscopy, and compared with appropriate standards (open circles). The analyses were performed using 1 mL of each cell suspension (in ultrapure water). The number of cells per mL was determined on sample aliquots, and the volume of a single cell was assumed as equal to 8 μm^3. It should be noted that the cells volume accounted for about 0.1% of the sample volume. To avoid underestimation of the Mn^{2+} concentration in cells grown for 19 h in manganese-enriched medium, the sample was diluted 1:2 with ultrapure water.

Figure 1

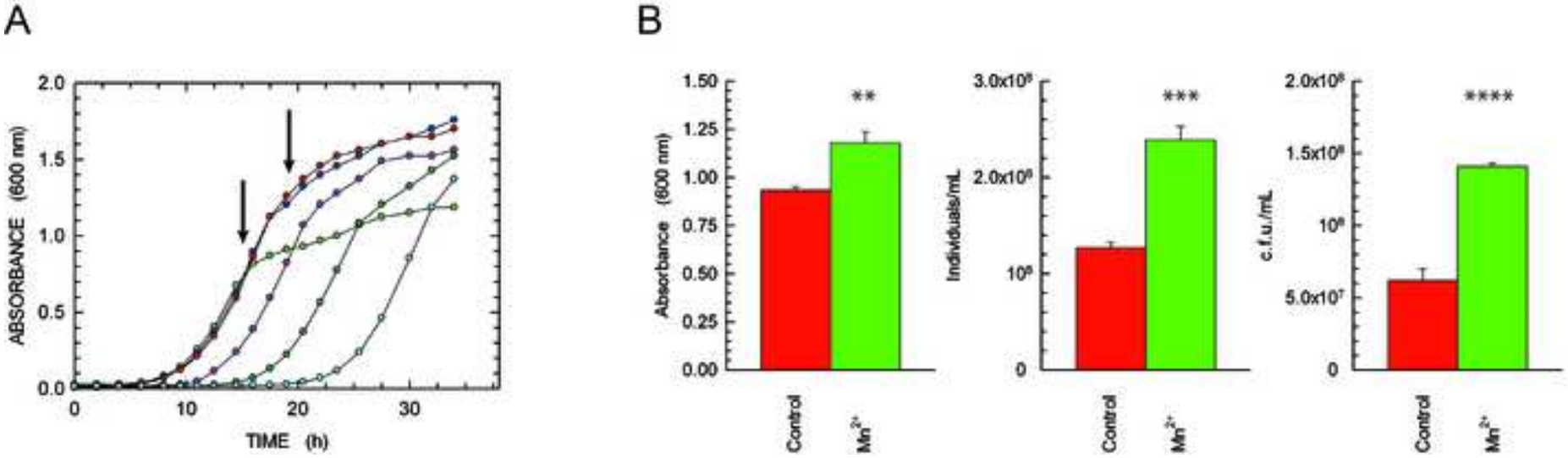
A
ABSORBANCE (600 nm)
TIME (h)
B
Absorbance (600 nm)
Individuals/mL
c.f.u./mL
**
***
****
Control
Mn2+

Figure 2

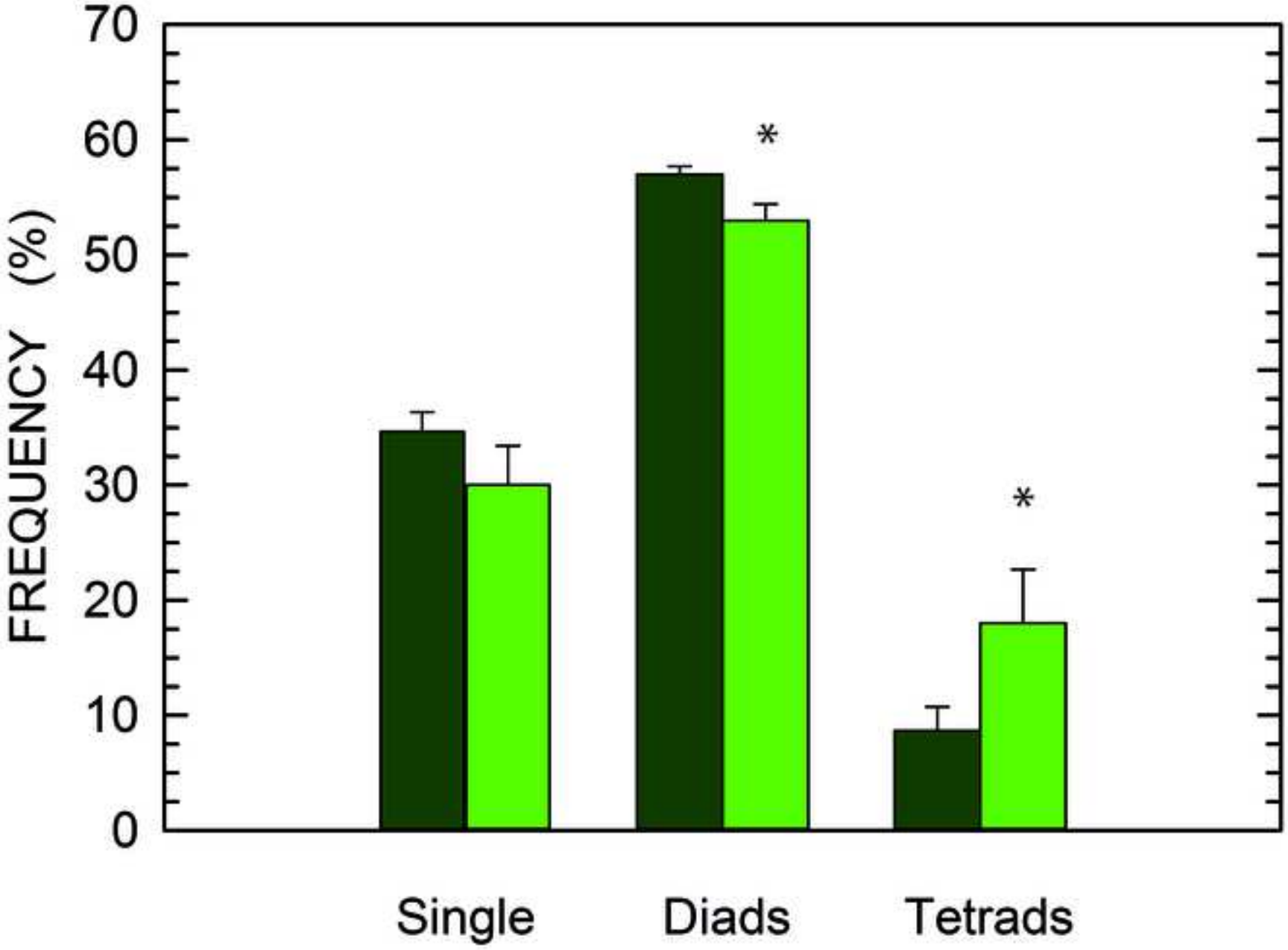

Figure 3

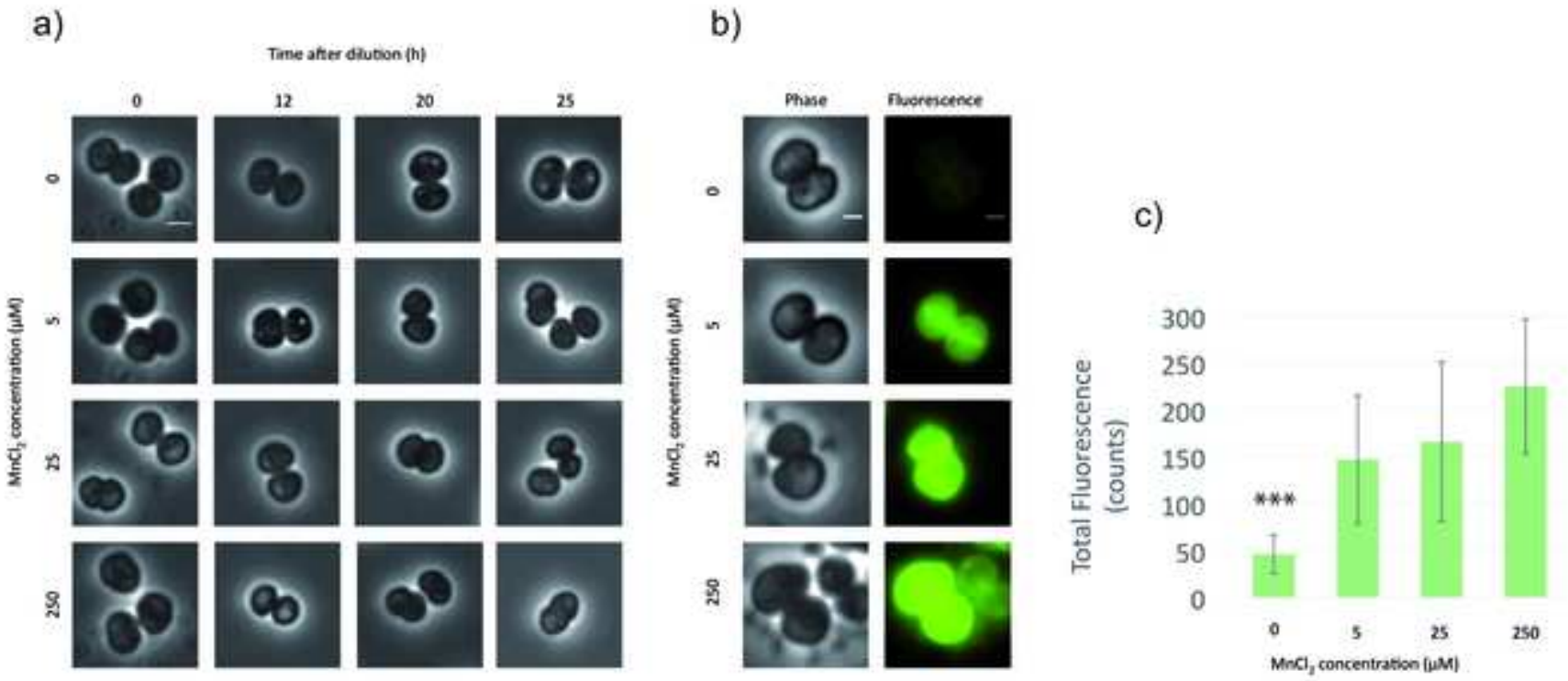
a)
Time after dilution (h)
0
12
20
25
$MnCl_2$ concentration (μM)
0
5
25
250
b)
Phase
Fluorescence
$MnCl_2$ concentration (μM)
0
5
25
250
c)
Total Fluorescence (counts)
300
250
200
150
100
50
0
***
0
5
25
250
$MnCl_2$ concentration (μM)

Figure 4

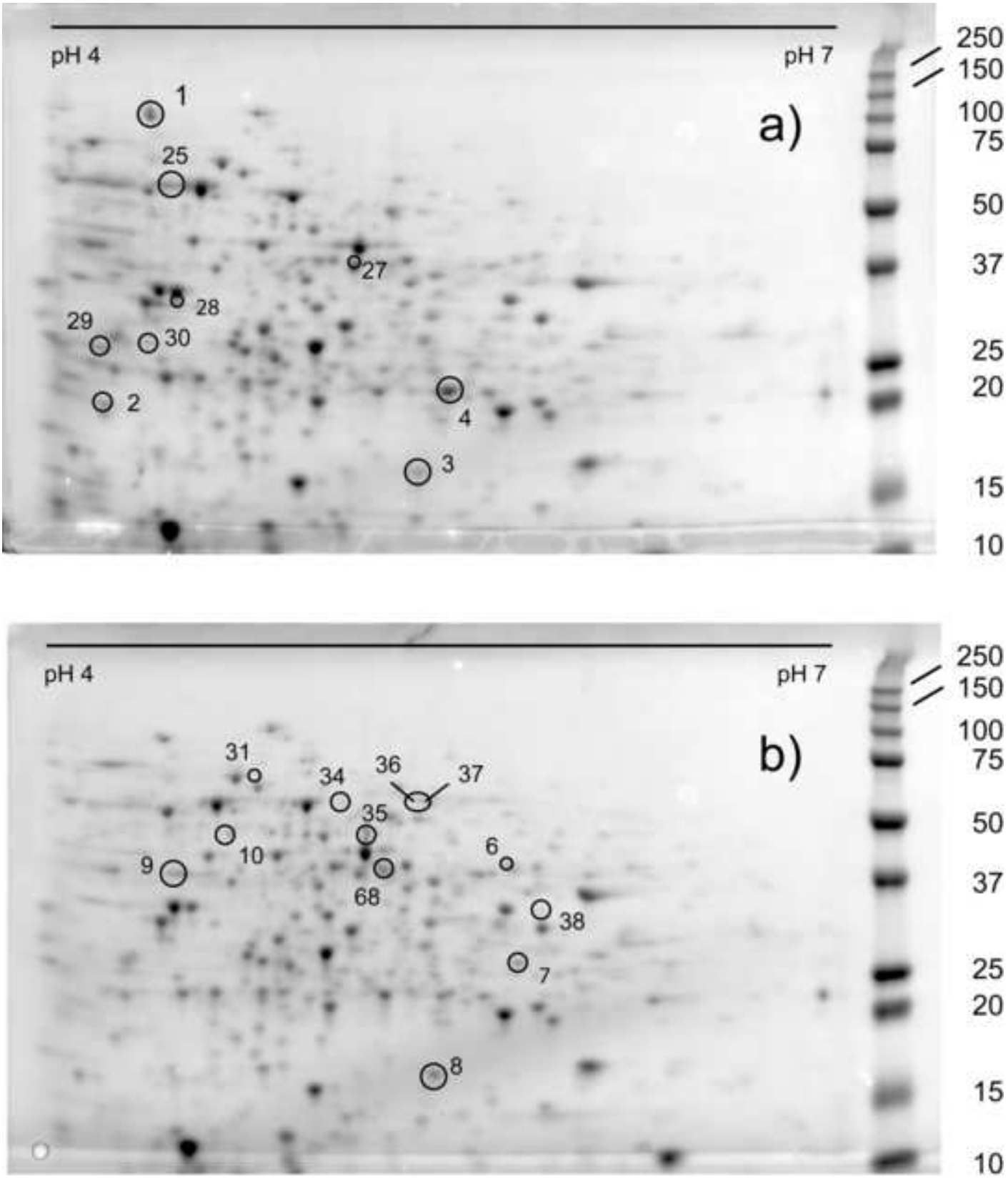
pH 4
pH 7
a)
1
25
27
28
29
30
2
4
3
250
150
100
75
50
37
25
20
15
10
pH 4
pH 7
b)
31
34
36
37
35
10
9
6
68
38
7
8
250
150
100
75
50
37
25
20
15
10

Figure 5

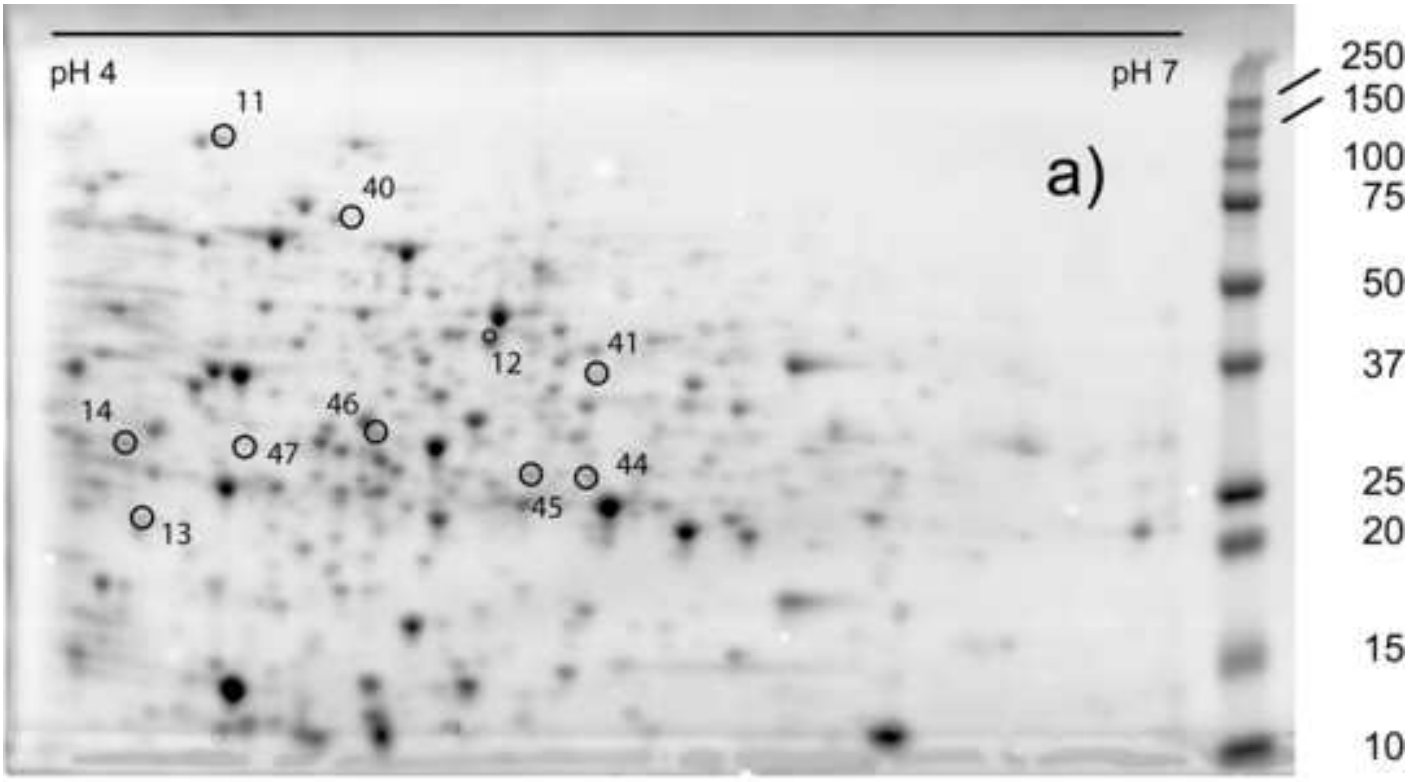
pH 4
pH 7
a)
11
40
12
41
14
46
47
44
45
13
250
150
100
75
50
37
25
20
15
10

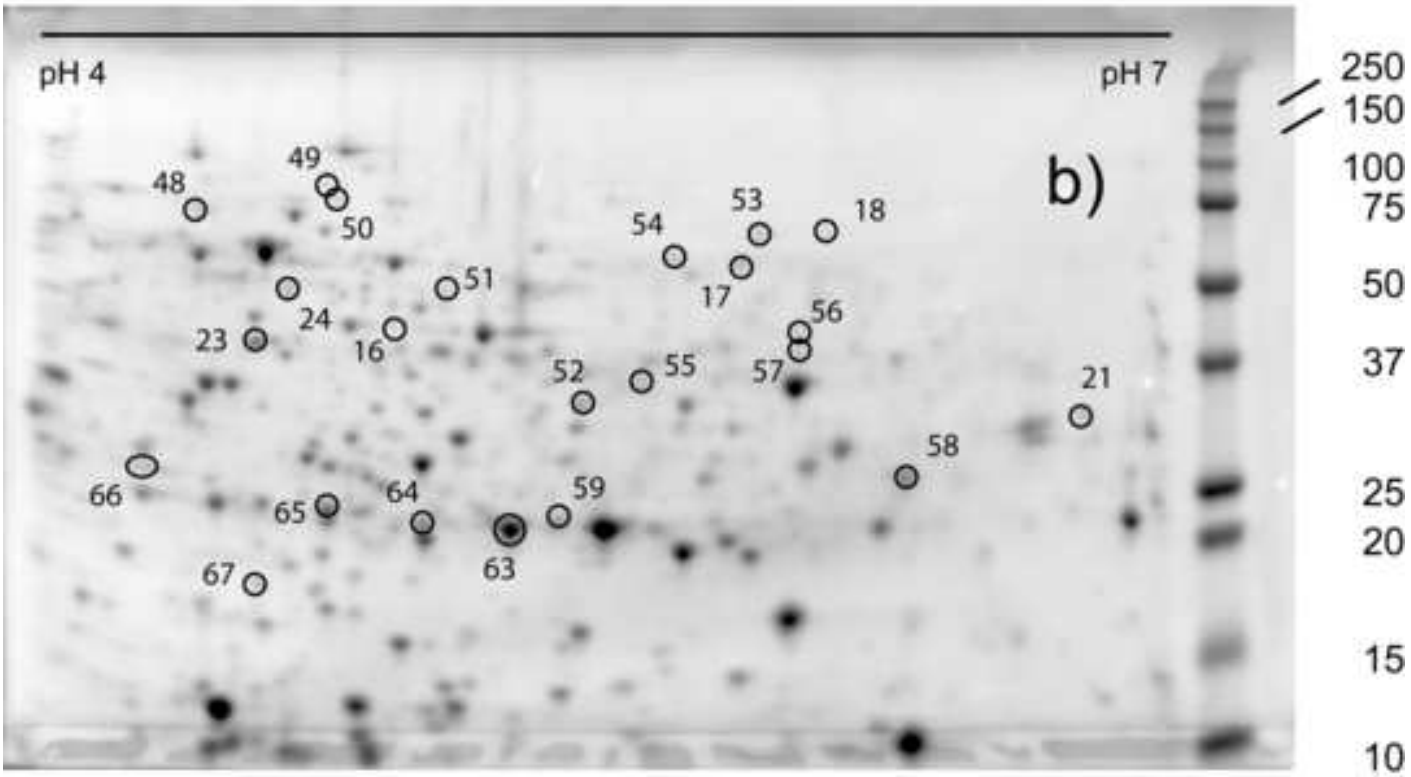
pH 4
pH 7
b)
49
48
50
53
18
54
17
51
24
56
23
16
52
55
57
21
58
66
64
59
65
63
67
250
150
100
75
50
37
25
20
15
10

Interval	Sample	Axis	Diameter	*n*
0 h	Control	2.73 ± 0.72	2.17 ± 0.38	213
	5 µM $MnCl_2$	2.76 ± 0.33	2.17 ± 0.36	246
	25 µM $MnCl_2$	2.77 ± 0.26	2.11 ± 0.33	217
	250 µM $MnCl_2$	2.76 ± 0.33	2.22 ± 0.33	247
12 h	Control	*2.81 ± 0.37	2.23 ± 0.21	328
	5 µM $MnCl_2$	2.74 ± 0.33	2.19 ± 0.20	252
	25 µM $MnCl_2$	2.70 ± 0.34	*2.11 ± 0.16	177
	250 µM $MnCl_2$	2.66 ± 0.29	*2.08 ± 0.18	450
20 h	Control	*2.88 ± 0.37	2.20 ± 0.23	217
	5 µM $MnCl_2$	2.73 ± 0.34	2.19 ± 0.21	242
	25 µM $MnCl_2$	2.70 ± 0.29	*2.10 ± 0.24	501
	250 µM $MnCl_2$	*2.64 ± 0.27	*2.06 ± 0.33	258
25 h	Control	*2.80 ± 0.36	2.11 ± 0.29	691
	5 µM $MnCl_2$	2.69 ± 0.36	2.11 ± 0.24	600
	25 µM $MnCl_2$	2.68 ± 0.37	2.10 ± 0.28	586
	250 µM $MnCl_2$	*2.59 ± 0.32	*2.05 ± 0.23	283

Table 1

Addition of Mn^{2+} to TGY medium and morphology of *D. radiodurans* cells. Measurements of cells axis and diameter of *D. radiodurans* cells incubated in the presence of 0 (control), 5, 25 or 250 µM $MnCl_2$ for 0, 12, 20 and 25 hours after dilution in TGY medium, at 30 °C. The experimental mean values were compared by the one-way ANOVA test (* indicates $P < 0.05$).

Identity	Function	Observed pI/Mr	
		-Mn	+Mn
Gi15807484 (DR_2499)	Nucleoside PPi kinase	**5.45/16** (spot 3)	**5.5/16** (spot 8)
Gi15807466 (DR_2480)	AcCoA Acetyltransferase	**5.25/40** (spot 27)	**5.36/40** (spot 68)
Gi15805338 (DR_0309)	Elongation factor Tu	**5.25/40** (spot 27)	**5.28/48** (spot 35)
Gi15807570 (DR_2588)	Iron ABC transporter	**4.38/27** (spot 30)	**5.78/26** (spot 7)
Gi15807039 (DR_2045)	50S ribosomal protein L1	**4.18/30** (spot 14)	**4.35/30** (spot 66)

Table 2

The addition of Mn^{2+} to TGY medium triggers a shift of the isoeletric points of some *D. radiodurans* proteins. Observed isoelectric points (pI) and molecular masses (Mr) of *D. radiodurans* proteins extracted from cells grown in TGY medium (-Mn) or in the same medium supplemented with 5 μM $MnCl_2$ (+Mn). The number of the spot from which proteins were extracted is indicated in brackets.